iris - AperTO

Dynamics of (4+1)-dihedrally symmetric nearly parallel vortex filaments

Paparella F. · Portaluri A.

Abstract We give a detailed analytical and numerical description of the global dynamics of $4 + 1$ points interacting through the singular logarithmic potential and subject to the following symmetry constraint: at each instant 4 of them form an orbit of the Klein group D_2 of order 4. The main device in order to achieve our results is to use a McGehee-like transformation introduced in [PaPo] for a problem analogous to the present one.

After performing this transformation in order to regularize the total collision, we study the rest-points of the flow, the invariant (stable and unstable) manifolds and we derive some interesting information about the global dynamics.

1 Introduction

The equations of motion of interacting point vortices were introduced by Helmholtz in a seminal paper published in 1858. In Helmholtz's view, point vortices on a plane actually were infinitely tall, infinitely thin, parallel vortex filaments perpendicular to the plane. Therefore, it was natural to ask questions about filaments which are not perfectly straight nor perfectly parallel. Based upon the equations governing the evolution of vorticity in a three-dimensional fluid, Da Rios in 1906 derived the localized self-induction approximation (LIA) describing the approximate motion of a weakly curved, isolated filament. The approximation was re-derived by Arms and Hama in 1965. Building on these results, Klein, Majda and Damodaran in [KlMaDa95] wrote a simplified model describing the time evolution of N-vortex filaments nearly but not perfectly parallel to the z-axis. According to this model the motion of N-interacting nearly parallel filaments is given by

Dr. Francesco Paparella
Dipartimento di Matematica, Università del Salento, Italy.
Tel.: +39-0832-297407
Fax: +39-0832-297410
E-mail: francesco.paparella@unisalento.it

Dr. Alessandro Portaluri
Dipartimento di Matematica, Università del Salento, Italy.
Tel.: +39-0832-297427
Fax: +39-0832-297410
E-mail: alessandro.portaluri@unisalento.it

the following coupled partial differential equations:

$$\frac{1}{i}\partial_t \Psi_j \;=\; \tilde{\Gamma}_j \partial_\sigma^2 \Psi_j + \sum_{k\neq j} \frac{\tilde{\Gamma}_k}{2\pi}\frac{\Psi_j - \Psi_k}{\|\Psi_j - \Psi_k\|^2} \tag{1}$$

for $j,k \in \{1,...,N\}$, $\tilde{\Gamma}_j \in \mathbb{R}^*$ and where each Ψ_j is a complex-valued function. Among all the solutions of the system (1) a special role is played by the *stationary solutions*.

In this paper we are interested in studying the geometry of the stationary solutions of (1). Therefore, by substituting in (1) $\Psi_j(\sigma,t)$ with $\boldsymbol{q}_j(\sigma)$, where $\boldsymbol{q} : \mathbb{R} \to \mathbb{R}^2$, we bring equations (1) down to the following system of coupled ordinary differential equations for stationary vortices filaments:

$$\tilde{\Gamma}_j \ddot{\boldsymbol{q}}_j(\sigma) + \sum_{k\neq j}\frac{\tilde{\Gamma}_k}{2\pi}\frac{\boldsymbol{q}_j(\sigma) - \boldsymbol{q}_k(\sigma)}{\|\boldsymbol{q}_j(\sigma) - \boldsymbol{q}_k(\sigma)\|^2} = 0 \tag{2}$$

where $\dot{\;}$ denotes differentiation with respect to the arc-length parameter σ.

By multiplying each equation in (2) by $\tilde{\Gamma}_j$ and defining the *potential function U* as

$$U(\boldsymbol{q}) := -\sum_{\substack{j=1\\k\neq j}}^{N}\frac{\tilde{\Gamma}_j\tilde{\Gamma}_k}{4\pi}\log\|\boldsymbol{q}_j - \boldsymbol{q}_k\| \tag{3}$$

where $\boldsymbol{q} := (\boldsymbol{q}_1,\ldots,\boldsymbol{q}_N)$, the ODE in (2) can be written as

$$\Gamma\ddot{\boldsymbol{q}} = \frac{\partial U}{\partial \boldsymbol{q}}. \tag{4}$$

Here Γ is the diagonal block matrix defined by $\Gamma = [\Gamma_{ij}]$ and $\Gamma_{ij} = \tilde{\Gamma}_i^2\delta_{ij}I_2$ where I_2 denotes the two by two identity matrix. By interpreting the parameter σ as a time-like coordinate, the equation (4) can be seen as describing the dynamics of point masses on the plane, interacting with a logarithmic potential. Therefore, from now on, we shall refer to the parameter σ as a *time-parameter*. A severe difficulty in investigating a system such as (4) is due to the presence of singularities both partial and total: physically they represent collisions between some or all of the vortices. This problem motivates the introduction of a change of coordinates that regularizes the equation of motion.

By using the change of coordinates studied in [PaPo], which mimics the change of coordinates introduced in 1974 by McGehee[McG74] in order to study collisions in the collinear three-body problem, we are able to derive some precise results about the global dynamics of our problem.

Summarizing, McGehee transformations consists of a polar-like change of coordinates in the configuration space, an energy-dependent rescaling of the momentum and a time scaling. The idea behind this non Hamiltonian change of coordinates is to blow-up the total collision to an invariant manifold called *total collision manifold* over which the flow extends smoothly. Furthermore, each hypersurface of constant energy has this manifold as a boundary. The effect of rescaling time, is to study some qualitative properties of the solutions close to total collision. In fact, by looking at the transformation defined in equation (9), it readily follows that the effect of this transformation is to slow the motion in the neighborhood of the total collapse, which is reached in the new time asymptotically. (For further details, please refer to [PaPo] and references therein).

In these new coordinates we were able to investigate the global dynamics of an example problem in which one vortex filament of strength γ is surrounded by four vortices, symmetrically arranged, having strength $\sqrt{\pi}$. For example, for $\gamma > -3\sqrt{\pi}/4$ we could prove that unbounded, collisionless orbits do not exist, and, conversely, for $\gamma < -3\sqrt{\pi}/4$ the equations of motion in McGehee coordinates immediately show how to find an unbounded, collisionless orbit. The value $\gamma = -3\sqrt{\pi}/4$ is, in fact, a threshold where the dynamics changes drastically. Above that threshold the center filament is attractive or weakly repulsive, and the total collision of all five vortices may happen. Below that threshold the repulsive strength of the central vortex does not allow the total collision. Results of this sort would be extremely difficult to prove by working in Cartesian coordinates.

In conclusion, we find that McGehee coordinates are a very important device for investigating this kind of singular problems. In addition to their importance from an analytical point of view, changes of coordinates of this sort may be play a crucial role in order to obtain accurate numerical approximations of the solutions close to total collapse, as their replace a horribly singular set of equations with one described by a smooth vector field.

2 McGehee coordinates and regularization

The aim of this section is to recall some facts about the McGehee–like transformation. The basic reference is [PaPo] and references therein.

2.1 General set-up and McGehee coordinates

Let $N \geq 2$ be an integer. Let $\mathbf{0}$ denote the origin in $\mathbb{R}^2$ and let $\tilde{\Gamma}_1, \ldots, \tilde{\Gamma}_N$ be N real numbers (which can be thought as strength of the vortex filaments). By the conservation law of the center of vorticity we can identify the configuration space $\boldsymbol{Q}$ for the problem with the subspace of $\mathbb{R}^{2N}$ defined by

$$\boldsymbol{Q} := \{\boldsymbol{q} = (\boldsymbol{q}_1, \ldots, \boldsymbol{q}_N) \in \mathbb{R}^{2N} : \ \sum_{j=1}^{N} \Gamma_j \, \boldsymbol{q}_j = \mathbf{0}\}.$$

For each pair of indexes $i, j \in \mathbf{N}$ let $\Delta_{i,j}$ denote the collision set of the i-th and j-th vortex filament; namely $\Delta_{i,j} = \{\boldsymbol{q} \in \mathbb{R}^{2N} : \boldsymbol{q}_i = \boldsymbol{q}_j\}$. We call *collision set* the subset of the configuration space given by $\Delta := \bigcup_{i \neq j} \Delta_{i,j}$ and *reduced configuration space*, the set $\hat{\boldsymbol{Q}} := \boldsymbol{Q} \setminus \Delta$. The Newton's equations in Hamiltonian form can be written as:

$$\begin{cases} \Gamma \dot{\boldsymbol{q}} = \boldsymbol{p} \\ \dot{\boldsymbol{p}} = \dfrac{\partial U}{\partial \boldsymbol{q}} \end{cases} \tag{5}$$

where the Hamiltonian function H is defined by:

$$H : T^*(\hat{\boldsymbol{Q}}) \longrightarrow \mathbb{R} \qquad H(\boldsymbol{q}, \boldsymbol{p}) := \frac{1}{2}\langle \Gamma^{-1} \boldsymbol{p}, \boldsymbol{p} \rangle - U(\boldsymbol{q}), \tag{6}$$

on the *phase space* $T^*(\hat{\boldsymbol{Q}}) = \hat{\boldsymbol{Q}} \times \boldsymbol{P}$ for

$$\boldsymbol{P} := \{\boldsymbol{p} = (\boldsymbol{p}_1, \ldots, \boldsymbol{p}_N) \in \mathbb{R}^{2N} | \ \sum_{j=1}^{N} \boldsymbol{p}_j = 0\}.$$

REMARK 1 *The differential equations in (5) then determine a vector field with singularities on $\mathbb{R}^{2N} \times \mathbb{R}^{2N}$, or a real analytic vector field without singularities on $(\mathbb{R}^{2N} \setminus \Delta) \times \mathbb{R}^{2N}$. The vector field given by (5) is everywhere tangent to $\boldsymbol{Q} \times \boldsymbol{P}$ and so this $4(N-1)$ dimensional linear subspace is invariant under the flow. We henceforth restrict our attention to the flow on the phase space $\boldsymbol{Q} \times \boldsymbol{P}$. Consequently H is an integral of the system. This means that the level sets $\Sigma_h := H^{-1}(h) \cap (\boldsymbol{Q} \times \boldsymbol{P})$ are also invariant under the flow (5). We observe that Σ_h is a real analytic submanifold of $\hat{\boldsymbol{Q}} \times \boldsymbol{P}$ having dimension $4(N-1) - 1$. The flow, however, is not complete. In fact certain solutions run off in finite time. This happens in correspondence to any initial condition leading to a collision between two or more vortex filaments: the corresponding solution meet Δ in finite time. We shall call* total collapse, *or* total collision *the simultaneous collision of all the vortices. Because the center of vorticity has been fixed at the origin, if a total collapse happens, it must occur at the origin of $\boldsymbol{Q}$.*

DEFINITION 2 *If $\hat{\boldsymbol{q}}_j := (\boldsymbol{q}_j, 0) \in \mathbb{R}^3$, $\hat{\boldsymbol{p}}_j := (\boldsymbol{p}_j, 0) \in \mathbb{R}^3$ then the* angular momentum *is defined as*

$$\boldsymbol{M}\,\boldsymbol{e}_3 \;=\; \sum_{j=1}^{N} \Gamma_j^{-1}\,(\hat{\boldsymbol{q}}_j \times \hat{\boldsymbol{p}}_j). \tag{7}$$

DEFINITION 3 *A point $\boldsymbol{s} \in \mathbb{R}^{2N}$, such that $\langle \Gamma \boldsymbol{s}, \boldsymbol{s} \rangle = 1$ is called* central configuration *if*

$$\frac{\partial U}{\partial \boldsymbol{q}}(\boldsymbol{s}) = \mu\,\Gamma\,\boldsymbol{s}, \qquad for\ some\ \ \mu \in \mathbb{R}.$$

By Definition 3 it follows that

LEMMA 4 *Let $\boldsymbol{s}$ be a central configuration, and ρ be a positive smooth function such that*

$$\ddot{\rho} = \mu \rho^{-1}.$$

Then $\boldsymbol{q}(\sigma) = \rho(\sigma)\,\boldsymbol{s}$ is a solution of (4).

Proof See [PaPo] for further details.   □

Let φ_1, φ_2 be the two monotonically increasing, smooth functions on the positive half-line, vanishing when $r \to 0^+$, defined by:

$$\begin{cases} \varphi_1(r) := r e^{-1/r^2} \\[2mm] \varphi_2(r) := r \end{cases} \tag{8}$$

We define the following McGehee-like coordinates:

$$\begin{cases} \|\boldsymbol{q}\| = \varphi_1(r) \\[2mm] \boldsymbol{s} = \boldsymbol{q}/\|\boldsymbol{q}\| \\[2mm] \boldsymbol{z} = \varphi_2(r)\boldsymbol{p}. \end{cases} \tag{9}$$

In these coordinates, it follows that a *total collapse* may only happen at $r = 0$. This constraint defines the *collision manifold*.

2.2 Equation of motions in $(r, \boldsymbol{s}, \boldsymbol{z})$- coordinates

In order to write the equations of motion using the McGehee coordinates, it will be useful to define $v := \langle \Gamma^{-1} \boldsymbol{z}, \boldsymbol{s} \rangle$ and to rescale time according to $e^{1/r^2}/r^2\, d\sigma = d\tau$. In these new coordinates the submanifold of constant energy h is given by

$$\Sigma_h = \left\{ (r, \boldsymbol{s}, \boldsymbol{z}) \in \mathbb{R}_+^* \times \boldsymbol{S} \times \mathbb{R}^2 \mid \langle \Gamma^{-1} \boldsymbol{z}, \boldsymbol{z} \rangle = 2r^2 \left[h + U(re^{-1/r^2}\boldsymbol{s}) \right] \right\}. \tag{10}$$

By taking into account the expression (3) for the potential, we get

$$r^2 U(re^{-1/r^2}\boldsymbol{s}) := -r^2 \left[\sum_{k \neq j} \frac{\tilde{\Gamma}_j \tilde{\Gamma}_k}{4\pi} \left(\log \varphi_1(r) + \log |\boldsymbol{s}_j - \boldsymbol{s}_k| \right) \right].$$

Moreover $1 := \lim_{r \to 0^+} -r^2 \log \varphi_1(r)$ and by this it follows that the stratum Σ_h meets the collision manifold $r = 0$ along the submanifold

$$\Lambda := \left\{ (0, \boldsymbol{s}, \boldsymbol{z}) \in \mathbb{R}_+^* \times \boldsymbol{S} \times \mathbb{R}^2 \mid \frac{1}{2} \langle \Gamma^{-1} \boldsymbol{z}, \boldsymbol{z} \rangle = G \right\},$$

where $G := \sum_{k<j} \dfrac{\tilde{\Gamma}_j \tilde{\Gamma}_k}{2\pi}$. We observe that Λ does not depend on the energy level h. Therefore, all strata Σ_h share the same boundary at the collision manifold. We also note that $\Lambda = \emptyset$ if $G < 0$. The Hamiltonian system (4) fits into the following

$$
\begin{cases}
r' = \dfrac{r^3}{r^2 + 2} v \\[2mm]
\boldsymbol{s}' = \Gamma^{-1} \boldsymbol{z} - v\boldsymbol{s} \\[2mm]
\boldsymbol{z}' = r^2 \left[\dfrac{1}{r^2 + 2} v\boldsymbol{z} + \dfrac{\partial U}{\partial \boldsymbol{q}}(\boldsymbol{s}) \right].
\end{cases}
\tag{11}
$$

where, in the last equation, we have used the identity $re^{-1/r^2} \partial_{\boldsymbol{q}} U(\boldsymbol{q}) = \partial_{\boldsymbol{q}} U(\boldsymbol{s})$.

3 The dihedral problem

Let us recall some basic facts about the dihedral group, seen as a map of $\mathbb{R}^2$ into itself. For further details we shall refer to [FePo08] or [PaPo]. Let $\mathbb{R}^2 \cong \mathbb{C}$ be endowed with coordinates $z \in \mathbb{C}$. For $l \geq 1$, let ζ_l denote the primitive root of unity $\zeta_l = e^{2\pi i/l}$; the *dihedral* group D_l is the group of order $2l$ generated by

$$
\zeta_l \colon z \mapsto \zeta_l z, \qquad \kappa \colon z \mapsto \overline{z},
$$

where $\overline{z}$ is the complex conjugate of z. The non-trivial elements of $D_l = \langle \zeta_l, \kappa \rangle$ are the $l-1$ rotations around the l-gonal axis ζ_l^j, $j = 1, \dots, l-1$ and the l rotations of angle π around the l digonal axes orthogonal to the l-gonal axis $\zeta_l^j \kappa$, $j = 1, \dots, l$. The action of D_l, restricted on the fixed subspace $\left(\mathbb{R}^{4l}\right)^{D_l} \cong \mathbb{R}^2$, generates a dihedral configuration of vortices for any given $\boldsymbol{q}_0 \in \mathbb{R}^2$.

We assume to have 4 vortices with the same circulation (which is a necessary condition in order to satisfy the symmetry constraint) $\tilde{\Gamma}_i^2 = 2\pi/l$ and another vortex of circulation γ placed at the center of vorticity. Then we can express the potential in terms of the coordinates of a single vortex, in the following way:

$$
U(\boldsymbol{q}_0) = - \sum_{g \in D_l \smallsetminus \{1\}} \log \|\boldsymbol{q}_0 - g\boldsymbol{q}_0\| - \sum_{g \in D_l} \frac{\gamma}{\sqrt{\pi}} \log \|g\boldsymbol{q}_0\|,
\tag{12}
$$

where, without further loss of generality, we have taken $\tilde{\Gamma}_i^2 = 2\pi/l$.

LEMMA 5 *The angular momentum of any dihedral equivariant orbit is zero.*

Proof See Lemma 2.1 in [PaPo] $\qquad\qquad\square$

For $l = 2$, the dihedral group is usually called *Klein group*. This is an abelian group of order 4. The *dihedral potential* in this case is given by:

$$
U(\boldsymbol{q}_0) = - \sum_{g \in D_2 \smallsetminus \{1\}} \log \|\boldsymbol{q}_0 - g\boldsymbol{q}_0\| - \sum_{g \in D_2} \frac{\gamma}{\sqrt{\pi}} \log \|g\boldsymbol{q}_0\|.
\tag{13}
$$

A straightforward computation shows that by setting $\boldsymbol{q} = (q_1, q_2)$ the potential may be written as

$$
U(q_1, q_2) = - \log(8\, q_1\, q_2\, \|\boldsymbol{q}\|) - \frac{4\gamma}{\sqrt{\pi}} \log \|\boldsymbol{q}\| = - \log(8 q_1 q_2 \|\boldsymbol{q}\|^{\beta+1}).
\tag{14}
$$

where we have defined $\beta = 4\gamma/\sqrt{\pi}$. In polar coordinates we have the following definition.

DEFINITION 6 *We define the* (4+1)*-dihedral logarithmic potential as :*

$$
U(\rho, \alpha) := - \log \rho^{\beta+3} - \log\left(4 \sin(2\,\alpha)\right),
\tag{15}
$$

and the (reduced) dihedral logarithmic potential *as:*

$$
U(\alpha) := - \log\left(4 \sin(2\,\alpha)\right).
\tag{16}
$$

LEMMA 7 *(Planar square) The dihedral problem admits exactly one (up to permutation of the vortices) central configuration, which is given by the vertices $(e^{(2k+1)\pi i/4}, 0)$ of a regular square.*

In terms of the local parameterization of the unit sphere $\boldsymbol{s}(\alpha) = (s_1, s_2) := (\cos\alpha, \sin\alpha)$ as follows

$$U(\boldsymbol{s}) = -\log(8s_1\, s_2) \tag{17}$$

where we set $q_j = s_j\|\boldsymbol{q}\|$ for $j \in \mathbf{2}$. From (10) let us define $\hat{E}(h, r, \boldsymbol{s}) := 2r^2(h + U(re^{-1/r^2}\boldsymbol{s}))$. More explicitly (see Figure 1) $\hat{E}$ is given by:

$$\hat{E}(h, r, \alpha, \beta) := 2\left[h\, r^2 + (\beta + 3)(1 - r^2\log r)\right] - 2r^2\log(4\sin(2\alpha)). \tag{18}$$
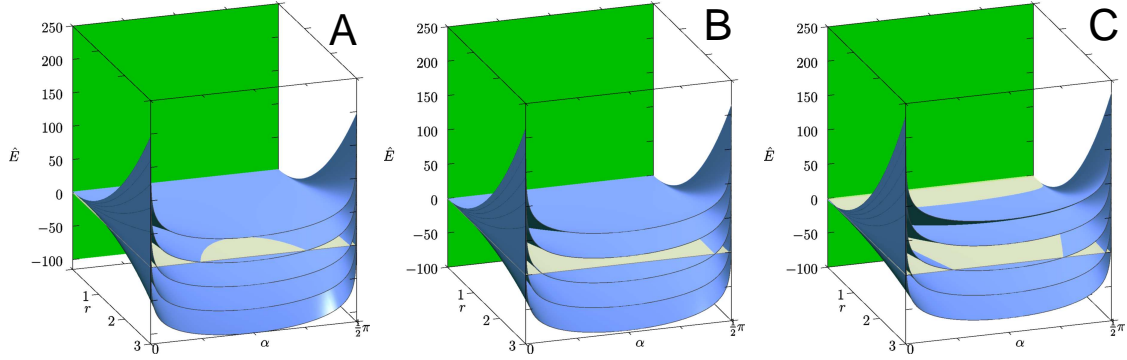
Therefore the hypersurface corresponding to the energy level h is given by

$$\Sigma_h = \left\{(r, \alpha, \boldsymbol{z}) \in \mathbb{R}_+^* \times (0, \pi/2) \times \mathbb{R}^2 \mid \langle \Gamma^{-1}\boldsymbol{z}, \boldsymbol{z}\rangle = \hat{E}(h, r, \alpha, \beta)\right\}. \tag{19}$$

We also observe that Σ_h meets the boundary $r = 0$ along a submanifold given by

$$\Lambda := \left\{(0, \alpha, \boldsymbol{z}) \in \mathbb{R}_+^* \times (0, \pi/2) \times \mathbb{R}^2 \mid \langle \Gamma^{-1}\boldsymbol{z}, \boldsymbol{z}\rangle = 2(\beta + 3)\right\}.$$

REMARK 8 *Since the first term defining Λ is a positive definite quadratic form, it implies that for $\beta < -3$ it is empty.*


Fig. 1 Energy hypersurfaces for $h = -4, -2, 0, 2, 4$ (starting from below). Panel A): $\beta = -2$; panel B): $\beta = -3$; panel C): $\beta = -4$. The white plane is the surface $\hat{E} = 0$ that separates the physically meaningful ($\hat{E} \geq 0$) from the physically meaningless ($\hat{E} < 0$) region of the phase space. Note that all the energy surfaces meet together at a line on the total collision manifold (the green plane in the figure), which is in the physically meaningless region for $\beta < -3$.

REMARK 9 *The boundary of the regions where the motion occurs is given by $\hat{E}(h, r, \alpha, \beta) = 0$; more precisely, since the kinetic term $\langle \Gamma^{-1}\boldsymbol{z}, \boldsymbol{z}\rangle$ is a positive definite quadratic form, for any fixed energy level h the motion is possible where:*

$$\hat{E}(h, r, \alpha, \beta) \geq 0.$$

The shape of the curve $\hat{E}(h, r, \alpha, \beta) = 0$ is key in order to understand the dynamics of our problem (see Figure 2). Note that, if $\beta > -3$ then $\lim_{r\to\infty} \hat{E} = -\infty$, and the motion is sandwiched between the collision manifold $r = 0$ and the zero-velocity manifold $\hat{E} = 0$; if $\beta < -3$ then $\lim_{r\to\infty} \hat{E} = \infty$, and the surface $\hat{E} = 0$ limits the allowed values of r from below. If $\beta = -3$ then the qualitative shape of the hypersurface definded by the function $\hat{E}$ depends on h. For $h > \log(4)$ the manifold $\hat{E} = 0$ coincides with $r = 0$; in this case the motion is allowed for any $r > 0$. For $h \leq \log(4)$ the zero-velocity set is given by the union of the surfaces $r = 0$, $\alpha = \arcsin(e^h/4)/2$ and $\alpha = \left(\pi - \arcsin(e^h/4)\right)/2$, and the motion may only happen for $0 < \alpha < \arcsin(e^h/4)/2$ or $\left(\pi - \arcsin(e^h/4)\right)/2 < \alpha < \pi$.
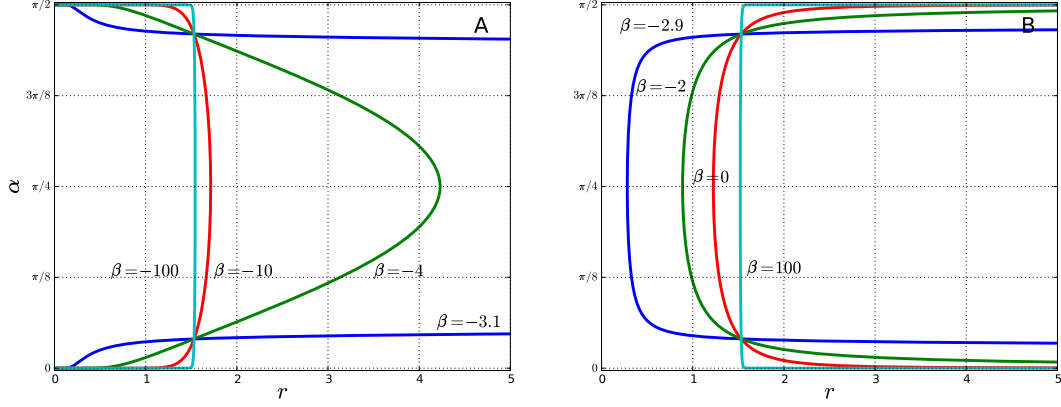
Fig. 2 Zero set of the function $(r, \alpha) \mapsto \hat{E}(0, r, \alpha, \beta)$ for several values of the parameter β. For $\beta < -3$ the physically meaningful region $\hat{E} > 0$ is on the right of the curves (panel A). For $\beta > -3$ it is on the left of the curves (panel B).

Let us introduce a further change of coordinates. In the dihedral problem the shape sphere reduces to S^1, therefore it is natural to use the parametrization $\alpha \mapsto \boldsymbol{s}(\alpha)$, where $\boldsymbol{s}(\alpha) = (\cos\alpha, \sin\alpha)$. Following [StFo03], we exploit the constraint (19) to parametrize the we also introduce a new local parametrization the momentum coordinates $\boldsymbol{z}$ with an angle ψ in the following way

$$\boldsymbol{z} = \sqrt{\hat{E}(h, r, \alpha)} \left(\sqrt{\pi}\cos\psi, \sqrt{\pi}\sin\psi\right). \tag{20}$$

Note that with the choice of the strength of the circulations made in Section 3, we have $\Gamma^{-1} = 1/\pi I$. We also use a new time-like variable ζ, define by $d\tau = \sqrt{\hat{E}}\, d\zeta$. Observing that the $(4+1)$-dihedral potential is given by:

$$U(\boldsymbol{q}) = -\log(8\|\boldsymbol{q}\|^{\beta+1} q_1 q_2)$$

by computing its gradient, we get:

$$\partial_{\boldsymbol{q}} U(\boldsymbol{q}) = -\left(\frac{1}{q_1} + (\beta+1)\frac{q_1}{\|\boldsymbol{q}\|}, \frac{1}{q_2} + (\beta+1)\frac{q_2}{\|\boldsymbol{q}\|}\right)$$

whence it follows $\partial_{\boldsymbol{q}} U(\boldsymbol{s}) = -\left(\dfrac{1}{s_1} + (\beta+1)s_1, \dfrac{1}{s_2} + (\beta+1)s_2\right)$. In this case the equations of motion become:

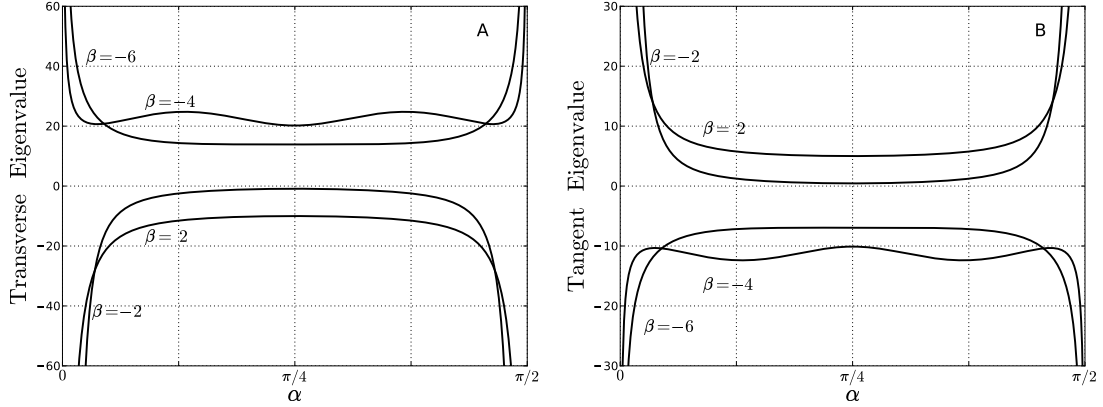$$\begin{cases} \dfrac{dr}{d\zeta} = \dfrac{1}{\sqrt{\pi}}\dfrac{r^3}{r^2+2}\, \hat{E}(h, r, \alpha, \beta)\, \cos(\psi - \alpha) \\[2mm] \dfrac{d\alpha}{d\zeta} = \dfrac{1}{\sqrt{\pi}}\hat{E}(h, r, \alpha, \beta)\, \sin(\psi - \alpha) \\[2mm] \dfrac{d\psi}{d\zeta} = \dfrac{-r^2}{\sqrt{\pi}}\left[\dfrac{2\cos(\psi + \alpha)}{\sin 2\alpha} - (\beta+1)\sin(\psi - \alpha)\right]. \end{cases} \tag{21}$$

The restpoints of (21) correspond to the solutions of the following systems:

$$\begin{cases} r = 0 \\ \sin(\psi - \alpha) = 0 \end{cases}, \qquad \begin{cases} r = 0 \\ \hat{E} = 0 \end{cases}, \qquad \begin{cases} \hat{E} = 0 \\ \dfrac{2\cos(\psi + \alpha)}{\sin 2\alpha} = (\beta+1)\sin(\psi - \alpha) \end{cases}.$$

However, it is readily seen that the second system has no solutions, as the conditions $\hat{E} = 0$ and $r = 0$ are incompatible. With straightforward calculations we obtain the following result.

Fig. 3 Eigenvalues of the rest points on the curve $\mathscr{P}_3$ for four distinct values of the parameter β. Panel A: eigenvalue corresponding to the eigenvector transverse to the surface $\hat{E} = 0$. Panel B: eigenvalues corresponding to the eigenvector tangent to the surface $\hat{E} = 0$, but transverse to the curve $\mathscr{P}_3$. Note the the third eigenvalue, namely that corresponding to the eigenvector tangent to the curve $\mathscr{P}_3$ is identically zero.

LEMMA 10 *The equilibria of the vector field given in* (21) *consists of four curves, two belonging to the collision manifold and the other two on the zero-velocity manifold. In the coordinates* (r, α, ψ), *the curves on the collision manifold are given by*

(i) $\mathscr{P}_1 \equiv (0, \alpha, \alpha)$;
(ii) $\mathscr{P}_2 \equiv (0, \alpha, \alpha + \pi)$

The curves on the zero-velocity manifold are given by

(iii) $\mathscr{P}_3$ *is the closure of the set* $\mathscr{P} \equiv \left\{ \left(\mathscr{R}(\alpha), \alpha, \arctan m(\alpha, \beta) \right) \mid \delta(\alpha, \beta) > 0, \ \alpha \in (0, \pi/2) \right\} \cup$ $\left\{ \left(\mathscr{R}(\alpha), \alpha, \arctan m(\alpha, \beta) + \pi \right) \mid \delta(\alpha, \beta) < 0, \ \alpha \in (0, \pi/2) \right\}$ *where*

$$m(\alpha, \beta) := \frac{\cos \alpha \left[(\beta + 1) \sin^2 \alpha + 1 \right]}{\sin \alpha \left[(\beta + 1) \cos^2 \alpha + 1 \right]}$$

$\delta(\alpha, \beta) := (\beta + 1) \cos^2 \alpha + 1$, *and the function* $\mathscr{R}$ *is implicitly defined by the equation* $\hat{E}(h, r, \alpha, \beta) = 0$, *which may be written as*

$$\log(4 \sin 2\alpha) = h + (\beta + 3)(r^{-2} - \log r);$$

(iv) $\mathscr{P}_4 \equiv \{ (r, \alpha, \psi + \pi) \mid (r, \alpha, \psi) \in \mathscr{P}_3 \}$.

Note that for $\beta = 1$ the ebove expressions for $\mathscr{P}_3$ and $\mathscr{P}_4$ become much simpler, namely $\mathscr{P}_3 = (\mathscr{R}(\alpha), \alpha, \pi/2 - \alpha)$ and $\mathscr{P}_4 = (\mathscr{R}(\alpha), \alpha, 3\pi/2 - \alpha)$.

The spectrum and the eigenvectors of the Jacobian matrix of (21), evaluated at a rest point, give useful information on the local dynamics close to the curves $\mathscr{P}_1$, $\mathscr{P}_2$, $\mathscr{P}_3$, $\mathscr{P}_4$. The logic of the calculation is elementary, but the computations become too large to be easily manageable. With the help of a computer algebra system (Maxima 5.21.1) we find the following results.

LEMMA 11 *The curves of equilibria* $\mathscr{P}_1$ *and* $\mathscr{P}_2$ *(on the collision manifold) given in Lemma 10 are degenerate. More precisely:*

1. *at each point of the curve* $\mathscr{P}_1$ *the spectrum is given by* $\mathfrak{s}(\mathscr{P}_1) = \{\lambda_1, \lambda_2\}$ *where* $\lambda_1 = (2\beta + 6)/\sqrt{\pi}$ *and* $\lambda_2 = 0$. *Furthermore the algebraic multiplicity of* λ_1 *is* $h(\lambda_1) = 1$ *and the algebraic multiplicity of* λ_2 *is* $h(\lambda_2) = 2$. *The eigenvectors are*

$$\boldsymbol{v}_1 = (0, 1, 0) \quad \boldsymbol{v}_2 = (1, 0, 0) \quad \boldsymbol{v}_3 = (0, 1, 1)$$

where $\boldsymbol{v}_1$ *is associated to* λ_1 *and* $\boldsymbol{v}_2$, $\boldsymbol{v}_3$ *are associated to* λ_2. *The vector* $\boldsymbol{v}_3$ *is tangent to* $\mathscr{P}_1$.

	$\dim W^s$	$\dim W^u$	$\dim W^0$
At $\mathscr{P}_1$	1	–	2
At $\mathscr{P}_2$	–	1	2
At $\mathscr{P}_3$	1	1	1
At $\mathscr{P}_4$	1	1	1

Table 1 Dimensions of the invariant manifolds for the equilibria belonging to the curves $\mathscr{P}_1$, $\mathscr{P}_2$, $\mathscr{P}_3$, $\mathscr{P}_4$ in the case $\gamma > -3/2$.

2. At each point of the curve $\mathscr{P}_2$ the spectrum is given by $\mathfrak{s}(\mathscr{P}_2) = \{\lambda_1, \lambda_2\}$ where $\lambda_1 = -(2\beta + 6)/\sqrt{\pi}$ and $\lambda_2 = 0$. The multiplicities and the eigenvectors are the same as for $\mathscr{P}_1$.

LEMMA 12 *For $\beta \neq -3$ the curves of equilibria $\mathscr{P}_3$ and $\mathscr{P}_4$ (on the zero velocity manifold) given in Lemma 10 are degenerate. More precisely:*

1. *at each point of the curve $\mathscr{P}_3$ the spectrum is given by three distinct simple eigenvalues, namely $\mathfrak{s}(\mathscr{P}_3) = \{\mu_1, \mu_2, \mu_3\}$ where*

$$\mu_1 = 0$$

$$\mu_2 = -\frac{1}{\sqrt{\pi}(\beta+1)}\left[128\cos(2\alpha)\cos(\psi+\alpha)r^8 e^{2(\beta\log(r)-\frac{\beta+3}{r^2}-h)} + 2(\beta+1)(\beta+3)\cos(\psi-\alpha)r^2\right]$$

$$\mu_3 = \frac{1}{\sqrt{\pi}}\left[8\sin(\psi+\alpha)r^5 e^{\beta\log(r)-\frac{\beta+3}{r^2}-h} + (\beta+1)\cos(\psi-\alpha)r^2\right],$$

and, for $\beta = -1$

$$\mu_2 = -\frac{1}{\sqrt{\pi}}\left[e^{\frac{2}{r^2}+h} + 16\cos^2(2\alpha)r^4 e^{-\frac{2}{r^2}-h}\right]$$

Here, of course, the coordinates are not independent, but $(r, \alpha, \psi) \in \mathscr{P}_3$. The eigenvector associated to μ_3 is $\boldsymbol{u}_3 = (0,0,1)$, which lies on the invariant manifold $\hat{E}(0, r, \alpha, \beta) = 0$. The explicit expressions of the eigenvectors $\boldsymbol{u}_1$ and $\boldsymbol{u}_2$ associated to μ_1 and to μ_2 are not short, and we omit them. However, $\boldsymbol{u}_1$ is tangent to the curve $\mathscr{P}_3$ and $\boldsymbol{u}_2$ is transverse to $\hat{E}(h, r, \alpha, \beta) = 0$. For $\beta > -3$ at all points in $\mathscr{P}_3$ we have $\mu_2 < 0$ and $\mu_3 > 0$. For $\beta < -3$ we have $\mu_2 > 0$ and $\mu_3 < 0$.

2. *At each point of the curve $\mathscr{P}_4$ the spectrum is $\mathfrak{s}(\mathscr{P}_3) = \{\mu_1, -\mu_2, -\mu_3\}$. The eigenvectors are the same as for $\mathscr{P}_3$.*

The dimension of all the stable, unstable and central manifolds associated to each rest point are shown in Table 1:

REMARK 13 *The above results show that for $\beta \neq -3$ the stability properties of the equilibria do not depend on the value of the total energy h. In other words, changing the parameter h does not lead to bifurcations.*

4 Heteroclinic connections, homothetic orbits and colliding trajectories

At each rest point let us denote by W^s, W^u respectively the (linearly) stable and unstable manifolds, and by W^0 the center manifold.

The existence of heteroclinic connections on and between the invariant manifolds helps us to develop a global understanding of the flow. For the proof of these results we shall refer to [PaPo].
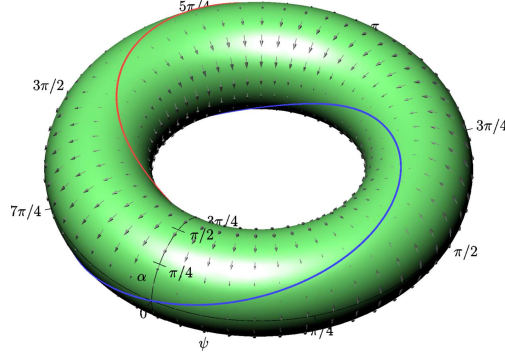
Fig. 4 Total collision manifold and equilibrium curves.

LEMMA 14 *The flow on the total collision manifold is* totally degenerate. *That is:*

(i) $W^u(\boldsymbol{P}_1) \equiv W^s(\boldsymbol{P}_2)$;
(ii) $W^u(\boldsymbol{P}_2) \equiv W^s(\boldsymbol{P}_1)$;

where $\boldsymbol{P}_1 \in \mathscr{P}_1$ and $\boldsymbol{P}_2 \in \mathscr{P}_2$ are chosen in such a way that the second coordinate of the two points is the same.

REMARK 15 *By taking into account the identification of the opposite edges of the rectangle (α, ψ) with the same orientation, the curves of equilibria can be identified with two closed curves on the torus and the heteroclinics are represented by arcs joining one point on a unstable (red) closed curve with the corresponding point on the stable (blue) curve as shown in Figure (4).*

Next we describe the flow on the zero velocity manifold $\hat{E}(h, r, \alpha, \beta) = 0$, where the equation of motions reduce to

$$\frac{dr}{d\zeta} = 0, \quad \frac{d\alpha}{d\zeta} = 0, \quad \frac{d\psi}{d\zeta} = -\frac{r^2}{\sqrt{\pi}} \left[\frac{2\cos(\psi + \alpha)}{\sin 2\alpha} - (\beta + 1)\sin(\psi - \alpha) \right]. \tag{22}$$

LEMMA 16 *The flow on the total collision manifold is totally degenerate. More precisely*

(i) $W^u(\boldsymbol{P}_3) \equiv W^s(\boldsymbol{P}_4)$;
(ii) $W^u(\boldsymbol{P}_4) \equiv W^s(\boldsymbol{P}_3)$;

where $\boldsymbol{P}_3 \in \mathscr{P}_3$ and $\boldsymbol{P}_4 \in \mathscr{P}_4$ are chosen in such a way the first two coordinates agree.

By choosing $(\alpha, \psi) = (\pi/4, \pi + \pi/4)$ or $(\alpha, \psi) = (\pi/4, \pi/4)$ the last two equations in (21) are identically zero. This means that the constant pair $(\alpha, \psi) = (\pi/4, \pi + \pi/4)$ is a constant solution of the subsystem obtained by projecting the system of ode's onto the (α, ψ)-plane. By summing up, the following result holds.

PROPOSITION 17 *There exist two heteroclinic orbits connecting the total collision and zero velocity manifold. More precisely*
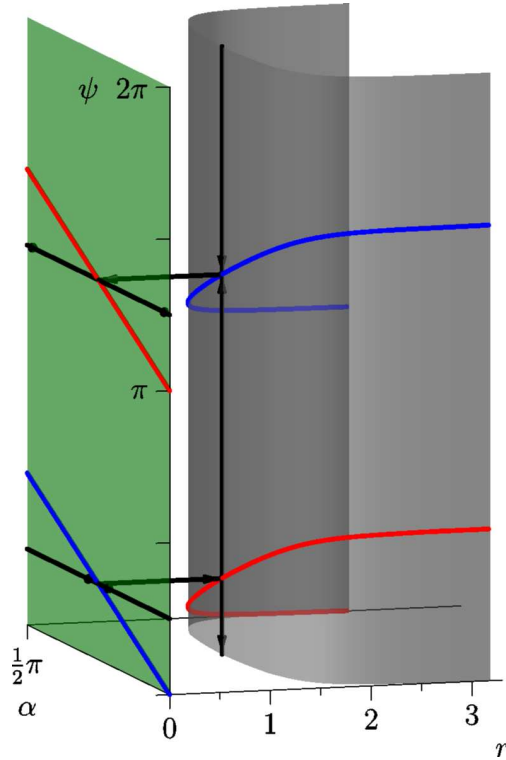
1. The curve $\eta_{13}(\zeta) = \big(r(\zeta), \pi/4, \pi/4\big)$ is an heteroclinic joining $\mathscr{P}_1$ and $\mathscr{P}_3$ for r solution of

$$\frac{dr}{d\zeta} = \frac{1}{\sqrt{\pi}} \frac{r^3}{r^2 + 2} \, \hat{E}(h, r, \pi/4, \beta).$$

2. the curve $\eta_{24}(\zeta) = \big(r(\zeta), \pi/4, \pi + \pi/4\big)$ is an heteroclinic joining $\mathscr{P}_4$ and $\mathscr{P}_2$ for r solution of

$$\frac{dr}{d\zeta} = -\frac{1}{\sqrt{\pi}} \frac{r^3}{r^2 + 2} \, \hat{E}(h, r, \pi/4, \beta).$$

where $\hat{E}(h, r, \pi/4, \beta) = 2\left[h\,r^2 + (\beta + 3)(1 - r^2 \log r)\right] - 2r^2 \log(4)$.

Fig. 5 Heteroclinic connections among the points $(0, \pi/4, \pi/4)$, $(0, \pi/4, \pi + \pi/4)$, $(\bar{r}, \pi/4, \pi/4)$, $(\bar{r}, \pi/4, \pi + \pi/4)$ where $\bar{r}$ is such that $\hat{E}(h, \bar{r}, \pi/4) = 0$. The shaded plane is the collision manifold $r = 0$. The shaded curved surface is the collision manifold $\hat{E} = 0$. Only the fundamental domain is shown. The figure was drawn for $\beta = 0$, and it is representative of all cases with $\beta > -3$.

REMARK 18 *Although mathematically the heteroclinics of Proposition 17 exist for any value of β, we should recall that the region of small values of r is physically reachable only for $\beta \geq -3$ owing to the constraint of Remark 8.*

Figure 5 shows graphically the heteroclinic connections between the invariant manifolds $r = 0$ and $\hat{E} = 0$.

5 Global dynamics in McGehee coordinates

DEFINITION 19 *We say that a solution $\gamma(\zeta) := (r(\zeta), \alpha(\zeta), \psi(\zeta))$ of the system (21) is unbounded if*

$$\lim_{\zeta \to +\infty} r(\zeta) = +\infty$$

If an orbit is not unbounded, then it is a rest point or it asymptotically approaches either a rest point or a collision.

The total collision of all five vortices may be only be achieved when $\beta > -3$, and by orbits that approach the heteroclinic orbit η_{24}. The latter statement is the consequence of a recent result [BaFeTe08] that generalizes to a large class of potentials (including logarithmic ones) the classic theorem by Sundman [Sun09], valid for Newtonian gravitational potentials, which states that total collisions may only be reached by approaching a *central configuration*. For more information on this issue, please refer to [PaPo].

The rest points on $\mathscr{P}_3$ and $\mathscr{P}_4$ are saddles. Only the orbits belonging to their stable manifold may asymptotically reach them. Therefore, the typical orbit is either unbounded, or it experiences a *binary collision*, defined as follows.

DEFINITION 20 *In a dihedrally equivariant system, a binary collision is the simultaneous, pairwise collision of all vortices whose position is different from the center of mass of the system.*

We have the following boundedness result.

THEOREM 21 *Unbounded collisionless orbit do not exist if $\beta > -3$.*

Proof $\boxed{\text{** TODO **}}$ □
For $\beta < -3$ or $\beta = -3$ and $h > \log(4)$, unbounded, collisionless orbits are possible. The simplest examples are the orbits generated by the equation that for $\beta > -3$ defines the heteroclinics η_{13} (see Proposition 17). However, we conjecture that these are not generic, in the following sense.

CONJECTURE 22 *For $\beta < -3$ or $\beta = -3$ and $h > \log(4)$ the set of initial conditions that generates unbounded, collisionless orbits has zero Lebesgue measure.*

The ubiquity of binary collisions motivates us to use the regularization techniques introduced in [CaTe] and further discussed in [PaPo], in order to introduce *generalized solutions*, which, roughly speaking, are suitable continuations of the solutions after a binary collision.
In physical coordinates, let us consider, in place of the singular potential (12), the non-singular one given by

$$U(\boldsymbol{q}_0; \varepsilon) = - \sum_{g \in D_l \smallsetminus \{1\}} \log \left(\sqrt{\|\boldsymbol{q}_0 - g\boldsymbol{q}_0\|^2 + \varepsilon^2} \right) - \sum_{g \in D_l} \frac{\gamma}{2} \log \sqrt{\|g\boldsymbol{q}_0\| + \varepsilon^2}, \qquad (23)$$

that substitutes (12) in the equations of motion (5). For the Klein group D_2 the above expression reduces to

$$U(q_1, q_2; \varepsilon) = \frac{1}{2} \log \left((4q_1^2 + \varepsilon^2)(4q_2^2 + \varepsilon^2)(4 \|\boldsymbol{q}_0\|^2 + \varepsilon^2)4(\|\boldsymbol{q}_0\|^2 + \varepsilon^2)^{\gamma/2} \right). \qquad (24)$$

It can be shown [CaTe,PaPo] that, in the limit $\varepsilon \to 0$, the solutions generated by the non-singular potential (23), at least in a finite time interval, become *transmission solutions*, which are continuous curves that locally obey the odd symmetry $\boldsymbol{q}_0(t_c + t) = -\boldsymbol{q}_0(t_c - t)$, where t_c is an instant of binary collision.
The non-singular potential (24) will be used below in order to compute numerical approximations to the generalized solutions.
For $\beta = 0$, is it possible to show [PaPo] that there are no unbounded generalized orbits. This result generalizes immediately to the case $\beta > 0$, and it is false in the case $\beta < -3$. We speculate that there is a regime in which both the collision manifold and infinity are dynamically accessible.

CONJECTURE 23 *There exists a constant $-3 < \beta^* < 0$ such that for $\beta < \beta^*$ there exist unbounded generalized solutions.*

6 Numerical Simulations

From now own, when we refer to *solutions* we mean *generalized solutions* that may go through binary collisions. The transformations linking the physical coordinates (q_1, q_2) and momenta (p_1, p_2) to the McGehee coordinates (r, α, ψ), for a given value of the total energy h, are

$$\begin{cases} q_1 = r \, e^{-1/r^2} \cos \alpha \\ q_2 = r \, e^{-1/r^2} \sin \alpha \end{cases} \qquad (25)$$

$$\begin{cases} p_1 = z_1/r = \sqrt{\hat{E} \, \pi}/r \, \cos \psi \\ p_2 = z_2/r = \sqrt{\hat{E} \, \pi}/r \, \sin \psi \end{cases} \qquad (26)$$
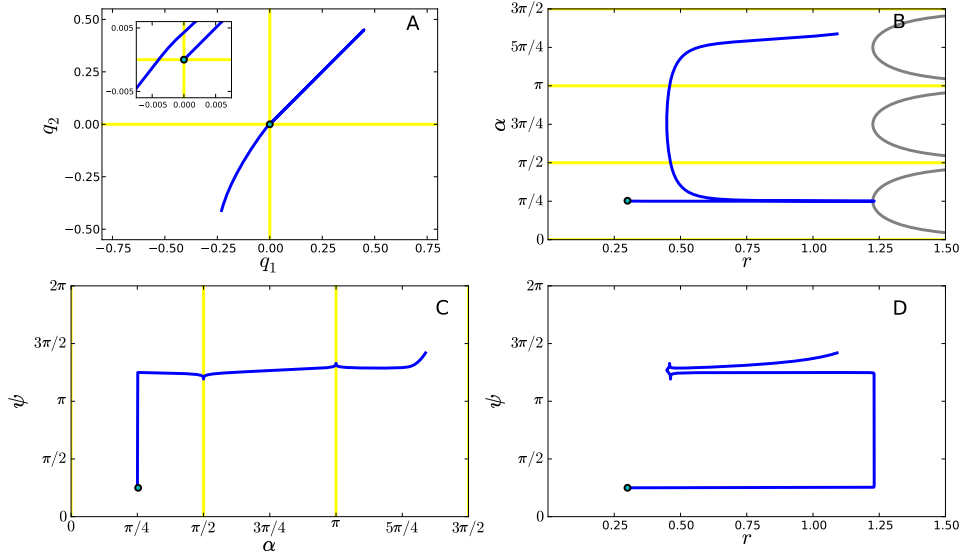
Fig. 6 A near-ejection orbit starting at $(r, \alpha, \psi) = (0.3, \pi/4 + 10^{-2}, \pi/4)$ with $h = 0$. The initial conditions are transformed to physical coordinates using equations (25) and (26), then a numerical integration of the equations (5) with the potential (24) and $\epsilon = 10^{-6}$ generates the orbit. Panel A): the orbit in physical coordinates, projected on the (q_1, q_2) plane. The inset magnifies the region close to the origin (corresponding to the total collapse). Panels B), C), D): the orbit transformed back to McGehee coordinates, projected respectively on the r, α, α, ψ, and r, ψ planes. After each binary collision the orbit is extended with continuity into the adjacent domain. The circle shows the position of the initial condition. The yellow lines at $\alpha = 0, \pi, \cdots$ correspond to binary collisions at $q_1 = 0$, those at $\alpha = \pi/2, 3\pi/2, \cdots$ to binary collisions at $q_2 = 0$. The grey lines in panel B) are the points with $\hat{E} = 0$.

We recall that the various time scalings introduced along calculations have the effect that both the invariant manifold corresponding to the total collapse and that corresponding to zero velocity are reached asymptotically as the rescaled time goes to infinity.

We further observe that not all the restpoints on the total collision manifold have a physical meaning. Only the points $(r, \alpha, \psi) = (0, \pi/4, \pi/4)$ and $(r, \alpha, \psi) = (0, \pi/4, 5\pi/4)$ are physically relevant. They correspond to central configurations in which each vortex lies on the vertex of a square, having the barycenter at the origin and the vertices on the bisectrices of the coordinate axis. Thus the two heteroclinic connections of proposition 17 joining the total collision manifold and the zero velocity manifold correspond, respectively to the homographic ejection orbit from total collapse to the zero velocity manifolds and to the homographic collision from the zero velocity to the total collapse manifolds.

This is illustrated in Figure 6 by a numerical solution of the equations of motions in physical coordinates using the non-singular potential (24) for an initial condition close to the ejection heterocline. Initially the solution follows closely the heteroclinic cycle shown in figure 5. Eventually, the solution leaves the collision heterocline before reaching the total collapse (which is a saddle point) and it is subject to a sequence of two binary collisions close to total collapse.

Summarizing we have

THEOREM 24 *The only homothetic ejection/collision orbit from/to total collapse is that homothetic to the planar central configuration, which is bounded.*

THEOREM 25 *Each solution different from the homothetic central configuration experiences a binary collision in finite time. Moreover, any solution starting arbitrarily close to the homothetic ejection solution has an orbit that may not reach the upper bound of the homothetic orbit before experiencing a binary collision.*
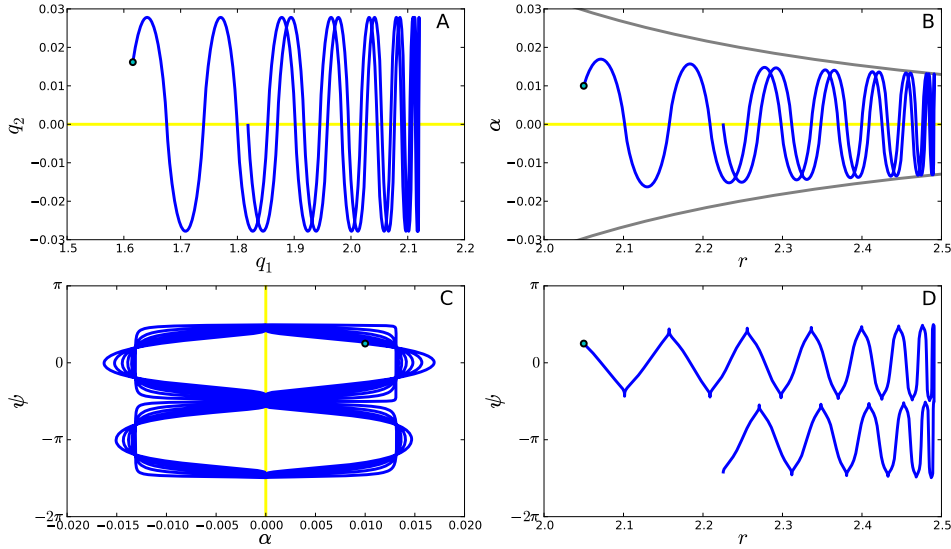
Fig. 7 A sequence of binary collisions moving along the positive q_1 semi-axis with a turning point. The orbit starts at $(r, \alpha, \psi) = (2.05, 0.01, \pi/4)$ with $h = 0$. Details of the numerical solution and panel description as in figure 6.

Proof This is a direct consequence of the theorem **??**.   □

When the four vortices are arranged at the vertex of a rectangle with a large ratio of side lengths, then there are solutions in which the pairs of vortices undergo repeated binary collisions along the same axis. In particular, for some of these solutions the sequence of collisions initially moves away from the origin of the Cartesian axes. However, unbounded solutions are not possible, and eventually the sequence reaches a turning point and returns towards the origin. An example of this dynamical behavior is shown in figure 7. When seen in the McGehee coordinates, these are solutions advancing (up to a turning point) into the narrow funnel between the zero velocity manifolds of adjacent domains. In figure 8 we show a numerical solution where a sequence of binary collisions approaching the origin from the right undergoes a single binary collision along the q_2 axis and the continues moving leftward on the negative q_1 semi-axis, although with a markedly different amplitude. Eventually, this it will reach a turning point, and return towards the origin. Solutions that oscillate along an axis bouncing back and forth between turning points of opposite sign are not uncommon. However, we were unable to maintain the oscillations, which are aperiodic, for arbitrarily long times. Eventually the orbit spends some time winding closely around the origin at distances corresponding to values of r such that $\hat{E}(h, r, \alpha) > 0$ for any α. After these complicated and chaotic-looking transients the orbit may resume its oscillations along one (not necessarily the same) axis.

We may formalize these findings as follows.

THEOREM 26 *If the initial configuration is a rectangle with large enough aspect ratio, the configuration evolves by passing through an arbitrary number of simultaneous binary collisions between the pairs of closest vortices.*

THEOREM 27 *The projection of any solution in the configuration space is bounded.*

Proof This is a direct consequence of theorem 21.   □

THEOREM 28 *The set of initial conditions leading to total collapse or leading in an infinite amount of time to the outermost boundary region where the motion is allowed has zero Lebesgue measure.*
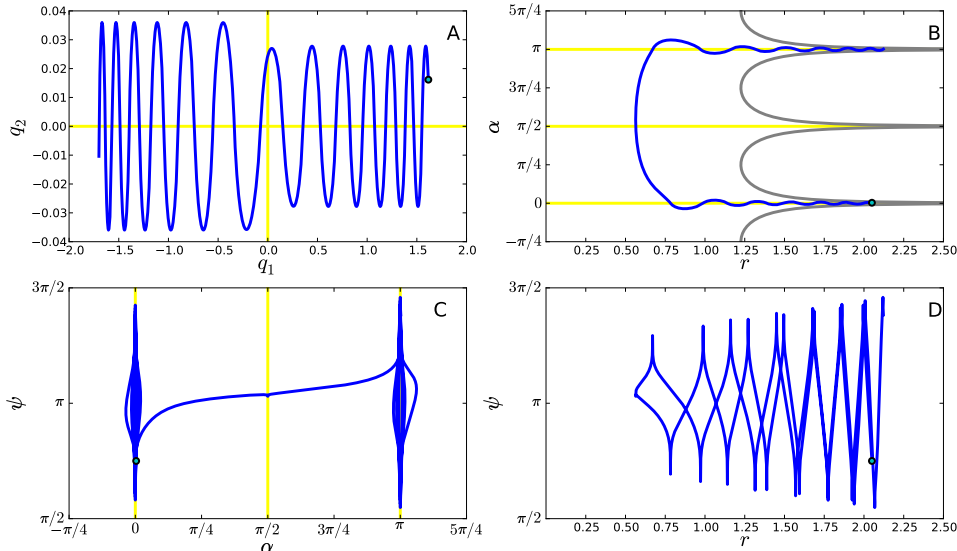
Fig. 8 A sequence of binary collisions moving from the positive to the negative q_1 semi-axis. The orbit starts at $(r, \alpha, \psi) = (2.05, 0.01, 3\pi/4)$ with $h = 0$. Details of the numerical solution and panel description as in figure 6.

References

[BaFeTe08] BARUTELLO, VIVINA; FERRARIO, DAVIDE L.; TERRACINI, SUSANNA On the singularities of generalized solutions to n-body-type problems. *Int. Math. Res. Not.* IMRN 2008.

[BaFuGr03] BELLETTINI G., FUSCO G:, GRONCHI G.F. Regularization of the two body problem via smoothing the potential *Commun. Pure Appl. Anal.*, 2 n. 3 (2003) 323–353.

[Cas05] ROBERTO CASTELLI Moti periodici di filamenti vorticosi quasi-paralleli Laurea Magistrale dissertation at University of Milano-Bicocca, 2004.

[Cas09] ROBERTO CASTELLI On the variational approach to the one and N-centre problem with weak forces. Ph.D. dissertation at University of Milano-Bicocca, 2009.

[CaTe] ROBERTO CASTELLI, SUSANNA TERRACINI On the regularization of the collision solutions of the one-center problem with weak forces To appear on Journal of Mathematical Analysis and Applications. http://arxiv.org/abs/0905.1579

[DeG96] DE GIORGI ENNIO Conjectures concerning some evolution problems. *Duke Math. J*, 81, n. 2 (1996), 255–268.

[DeVi99] DELGADO, J., AND VIDAL, C. The tetrahedral 4-body problem. *J. Dynam. Differential Equations 11*, 4 (1999), 735–780.

[Dev80] DEVANEY, R. L. Triple collision in the planar isosceles three-body problem. *Invent. Math. 60*, 3 (1980), 249–267.

[Dev81] DEVANEY, R. L. Singularities in classical mechanical systems. In *Ergodic theory and dynamical systems, I (College Park, Md., 1979–80)*, vol. 10 of *Progr. Math.* Birkhäuser Boston, Mass., 1981, pp. 211–333.

[Fer07] FERRARIO, DAVIDE L. Transitive decomposition of symmetry groups for the n-body problem. *Adv. in Math. 2* (2007), 763–784.

[FePo08] FERRARIO, DAVIDE L., PORTALURI, ALESSANDRO On the dihedral n- body problem. *Nonlinearity 21* (2008), 6 1307–1321.

[HiPuSh77] HIRSCH, M. W.; PUGH, C. C.; SHUB, M. Invariant manifolds. Lecture Notes in Mathematics, Vol. 583. Springer-Verlag, Berlin-New York, 1977

[KlMaDa95] KLEIN, RUPERT; MAJDA, ANDREW J.; DAMODARAN, KUMARAN Simplified equations for the interaction of nearly parallel vortex filaments. *J. Fluid Mech.* 288 (1995), 201–248.

[McG74] MCGEHEE, R. Triple collision in the collinear three-body problem. *Invent. Math. 27* (1974), 191–227.

[Moe81] MOECKEL, R. Orbits of the three-body problem which pass infinitely close to triple collision. *Amer. J. Math. 103*, 6 (1981), 1323–1341.

[Moe83] MOECKEL, R. Orbits near triple collision in the three-body problem. *Indiana Univ. Math. J. 32*, 2 (1983), 221–240.

[New01] NEWTON, PAUL The N-vortex problem. Analytical techniques. Applied Mathematical Sciences, 145. Springer-Verlag, New York, 2001.

[PaPo] Paparella, Francesco; Portaluri, Alessandro Global dynamics of the dihedral singular logarithmic potential and nearly parallel vortex filaments. *Submitted.* `http://arxiv.org/abs/1112.1789`

[Sun09] Sundman, K. F. Nouvelles recherches sur le probleme des trois corps. *Acta Soc. Sci. Fenn. 35*, 9 (1909).

[StFo03] Stoica, Cristina; Font, Andreea. Global dynamics in the singular logarithmic potential. *J. Phys. A* , 36 (2003), 7693–7714.

[Vid99] Vidal, C. The tetrahedral 4-body problem with rotation. *Celestial Mech. Dynam. Astronom. 71*, 1 (1998/99), 15–33.